Exploring Asymmetric Vent Designs in Loudspeaker Systems: A Combined COMSOL and Experimental Approach

Mithun Hari [1], Todd Michael [1]
1. Loudspeaker Design Lab, Yorkville Sound, Pickering, ON, Canada.

Abstract

Excessive vent noise poses a prevalent challenge in various acoustic applications, significantly impacting audio systems' performance and user satisfaction. This innovative research investigates the efficacy of noise reduction using a lumped speaker model implemented in COMSOL Multiphysics. The model integrates Electrical Circuit and Pressure Acoustics Physics to simplify speakers' intricate geometry and acoustic behavior into manageable equations. It is employed to simulate and analyze the acoustic characteristics of vented enclosures. Through systematic variations in vent flare and length parameters within the COMSOL environment, this study identifies key factors influencing noise generation and propagation.

Moreover, the study compares these findings with impedance testing of a prototype to assess vent tuning and associated noise at the tuning frequency. Simulation results provide crucial insights into the interactions among vent geometry, material properties, and the acoustic environment. The findings underscore that targeted modifications to vent design can effectively mitigate noise levels without compromising audio quality. This study offers a practical and applicable framework for optimizing vented speaker designs, delivering useful guidelines for engineers and designers seeking to enhance acoustic performance in consumer electronics, automotive sound systems, and similar applications.

Keywords: Loudspeaker Design, Lumped Parameters, Vent Geometry, Mechanical-Acoustic Coupling

Introduction

The loudspeaker design balances low-frequency enhancement with complexity management. Sealed-box speakers limit bass due to woofer suspension, causing distortion at high excursions. Bass reflex systems use a port as an MSD system, acting as a Helmholtz resonator to boost low frequencies but introduce issues like port noise and distortion. Since the 1970s, rounded or flared ports have mitigated these problems.

Research by Roozen [1,2,3], Backman [4], and Vanderkooy [5,6] shows that aerodynamic port design improves performance. By 1980, patents suggested flared port ends could be beneficial. Studies on pipe turbulence, like those by Ingard and Ising in 1967 [7] and Backman [4] in 1995, show slight port end curvatures reduce distortion. Roozen's work highlights the effectiveness of a gradual taper, with diagrams illustrating vortex behavior in ports.

Lumped Parameter Models have become integral in loudspeaker design, simplifying complex systems into manageable components. These models represent the loudspeaker's mechanical and acoustic behavior using electrical analogs, like mass, compliance, and resistance, which can be analyzed with circuit theory. This approach allows for quick predictions of system behavior, aiding in the design of bass reflex enclosures. Finite element analysis (FEA) in loudspeaker design simplifies components for quicker optimization, maintaining accuracy at High frequencies. This paper integrates bass reflex benefits with simplified FEA modeling for high-performance systems alongside lumped parameter models for initial design and optimization stages.

Vent Noise and Theory of Fluid Flow

In loudspeaker ports, airflow is treated as incompressible for velocities under 100m/s (Mach < 0.3), typical for loudspeaker use. The shift from laminar to turbulent flow in pipes generally occurs at a Reynolds number (Re) of 2300, but this threshold can rise with smoother or flared pipes. Turbulence in these ports can start at just 0.35 m/s, with practical Re limits reaching 100,000. Turbulence features chaotic, eddy-like movements where inertial forces overshadow viscous or buoyant forces, causing velocity fluctuations and noise up to 10kHz. It initiates when the inertial forces of vortices surpass the damping by viscous forces, leading to the growth of eddies.

At high Re, viscosity effects are confined to the boundary layer, where velocity transitions from zero at the wall to nearly the free stream speed over a short distance, about 1mm in ports. Flow speed increases while pressure drops in a converging boundary like a nozzle, creating a favorable pressure gradient. In contrast, a diverging boundary, such as a flared port's exit, slows the flow, increases pressure, and can lead to flow separation if the flare angle is too acute due to insufficient flow momentum.

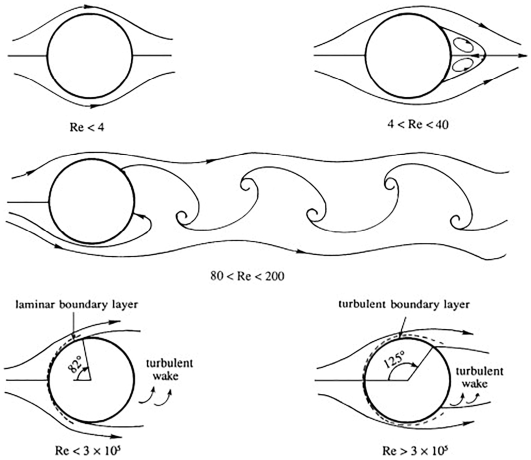

Figure 1. From Top Left Clockwise: No separation, Steady separation bubble, Oscillating Karman Vortex Street wake, Laminar Boundary Turbulent Boundary

This separation results from an overly strong adverse pressure gradient, causing local flow reversal and vortex formation, dissipating acoustic energy into friction instead of sound. Turbulent boundary layers are advantageous as they can resist higher adverse pressure gradients without separating [Figure 1], thanks to increased wall shear stress and momentum. Conditions like free stream disturbances, surface roughness, or vibrations can promote a transition to turbulence, which can be beneficial in preventing flow separation.

Vortex shedding, where flow detaches from surfaces forming eddies [Figure 1], is prominent at the rapid cross-sectional changes in flared tubes. This creates the von Kármán vortex street [Figure 1], where vortices alternate from each side of the tube, influenced by flow speed, tube diameter at separation, and fluid properties [8]. This shedding contributes to aerodynamic noise, reducing efficiency in loudspeakers by potentially causing fewer adequate bass or higher distortion and introducing flow instabilities, which are generally undesirable in controlled settings like speaker design.

Lumped Loudspeaker Model

A lumped model is suitable for analyzing speaker drivers where components move in a piston-like manner. This model is typically accurate at lower frequencies where the driver's size is significantly smaller than the sound wavelength. An Electromechanical or Electroacoustic model uses either small-signal (Thiele-Small parameters) for minor movements or large-signal parameters for significant movements. It provides an electrical circuit analogy that captures electrical and mechanical behaviors, facilitating interaction between the speaker and its acoustic surroundings.

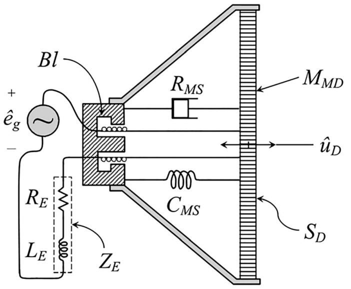

Figure 2. Classical Moving Coil Loudspeaker Model [10]

T-S (Thiele-Small) parameters are critical for our current study, as we are working on a production model with specific manufacturer drivers. The speaker's T-S parameters are then represented as lumped elements in an electrical circuit model in COMSOL [11]. This includes the voice coil and magnetic components in the electrical aspect (Figure 2), the mass of the voice coil and cone in the mechanical aspect, and the spring and damping effects from the suspension system in the mechanical aspect. Figure [3] shows the speaker driver components and the analogous circuit that are used in the COMSOL model for the study.

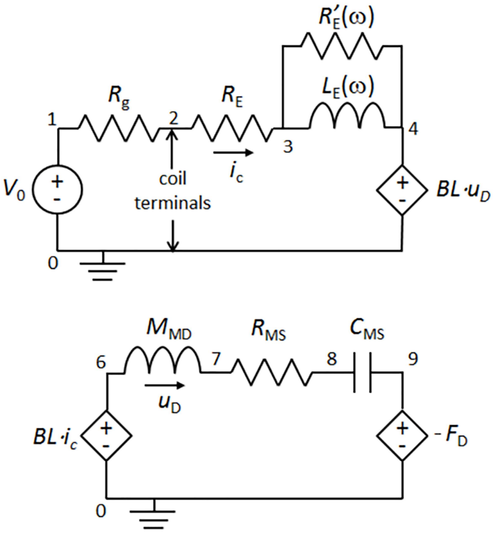

Figure 3. The lumped (circuit) representation for the electrical (top) and mechanical (bottom) components of the speaker driver. [12]

Loudspeaker Topology

This study is centered on a 30-liter subwoofer box equipped with a 10-inch driver. Our goal is to design the box with a smaller footprint in terms of width and depth while still maintaining a larger volume. The intention is to reduce manufacturing costs by using the same parts for different products, such as those with a 12-inch driver, achieved by keeping the width and depth consistent.

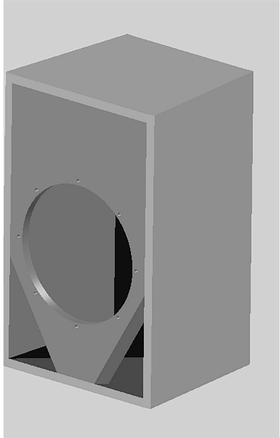

Figure 4. 30L wooden cabinet 3D model for prototype

An initial topology simulation uses LspCAD 5.25 [12] to finalize the vent tuning. Lavoce SSF102.50 4-ohm drivers are used to simulate the box. A decent SPL response is generated with a tuning of 52 Hz, Figure [5]. A 30-litre internal volume cabinet is designed using IronCAD 2024 [14], Figure [4]. Corner vents are finalized for the design as they give maximum volume and ease of installation and support the bottom of the cabinet and the gable.

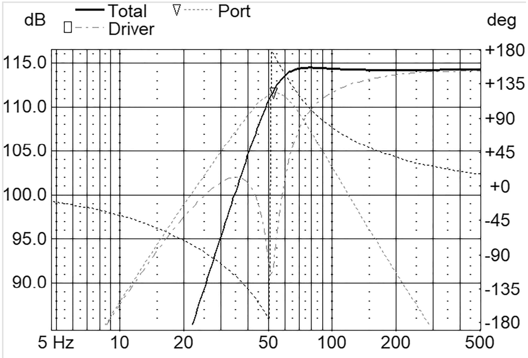

Figure 5. Simulated SPL response from LspCAD

Asymmetric Vent Design

The primary factors influencing the tuning of a port are its length and the minimum throat diameter. When the port's flare increases, traditional methods of calculating end correction, which rely on the radius at the port's mouth, tend to overestimate the reactive mass of air. A more accurate approach for predicting tuning involves using the minimum throat diameter rather than the maximum for calculating length corrections. Salvatti [10] analyzed the experimentally derived tuning frequencies about the flare radius, and a strong linear correlation (r^2=0.98) was observed between the Normalized Frequency Ratio (NFR) and the effective port area.

$$NFR = \frac{port_{leng}}{2\ x\ (flare_{radius})}$$

In our study, we applied the formula derived from Salvatti's [10] research to estimate the tuning frequency for a flared port. Initially, we designed the port with a fixed length of 7 inches, aiming for a Normalized Frequency Ratio (NFR) near 1.0. Given the constraint of the box's internal width, which measures 11.2 inches, we could not maintain symmetry in the port's dimensions along its height. Consequently, the port design became asymmetric, as Figure [6] depicts. This adjustment was necessary to accommodate the physical dimensions of the enclosure while still achieving the desired acoustic properties.

COMSOL Simulation Setup

The design of the asymmetric flared port was executed, utilizing the loft feature to create the port's complex geometry. The 3D asymmetric vent shape is placed inside the 30L cabinet, and the model was imported to COMSOL.

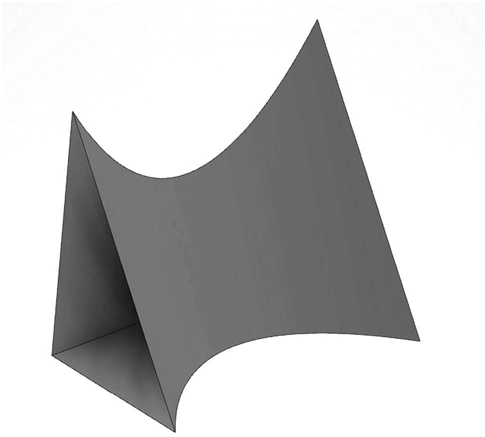

Figure 6. Asymmetric 3D vent model for COMSOL

In the COMSOL Multiphysics environment, the 10-inch woofer was represented using an interior lumped speaker boundary condition, simplifying the modeling of complex acoustic sources by treating the speaker as a point source within the enclosure, Figure [7]. A Symmetric Boundary Condition was applied to optimize computational efficiency, effectively halving the simulation domain and thus significantly reducing the computational load and time required for the analysis.

All internal enclosure surfaces, including the vent, were defined as interior sound rigid boundaries. This boundary condition assumes that the walls are perfectly rigid and reflective.

Figure 7. COMSOL Model

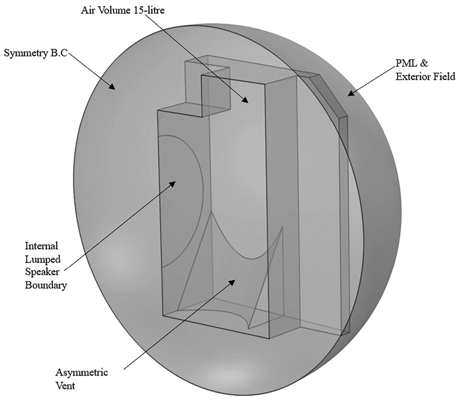

System Impedance Comparison

Impedance measurements are typically performed to check the system tuning. To validate the accuracy of our COMSOL Multiphysics simulation, we 3D printed (Figure [14]) the flared vents and measured the subwoofer's impedance using the Audio Precision APx515 audio analyzer [15], which is renowned for its precision in audio measurements. The impedance data obtained from these measurements were then compared with the impedance curves generated by COMSOL.

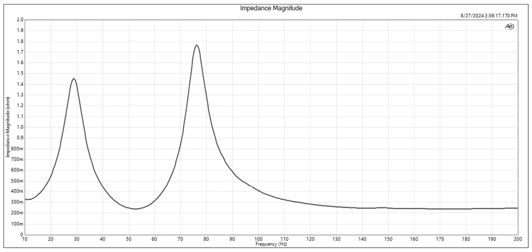

Figure 8. 3D printed flared vent Impedance measurement by APx515 Analyzer

The results from both sources demonstrated a high degree of correlation at the tuning frequency, i.e., 52 Hz ± 2 Hz, affirming the reliability of our COMSOL model in predicting real-world impedance behavior. This close alignment between simulation and physical measurement validates the COMSOL study and underscores the model's capability to simulate complex acoustic and electrical interactions within the subwoofer system.

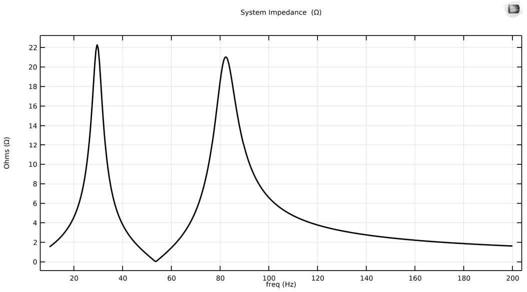

Figure 9. 3D printed flared vent Impedance measurement from COMSOL.

We also utilized LspCAD 5.25 for an initial impedance simulation, specializing in loudspeaker design. The impedance profile from LspCAD closely matched the COMSOL simulations and the experimental data gathered from the APx515 audio analyzer. This three-way validation, encompassing COMSOL, LspCAD, and real-world measurements, confirms that our simulation techniques accurately capture the subwoofer's impedance behavior across its frequency range.

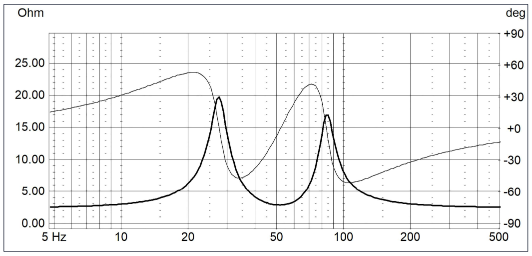

Figure 10. 3D printed flared vent Impedance simulated from LspCAD.

Acoustic Velocity Comparison

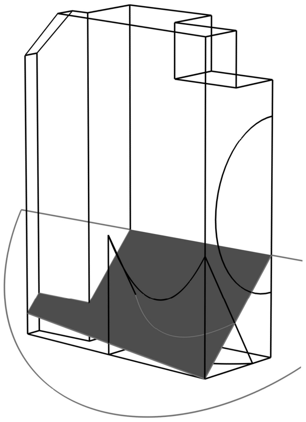

Figure 11. Cut Plane Data set on COMSOL to plot velocity contour

Acoustic velocity in the subwoofer vent is plotted for the flared asymmetric port and the straight port through a cut plane through the ports [Figure 11].

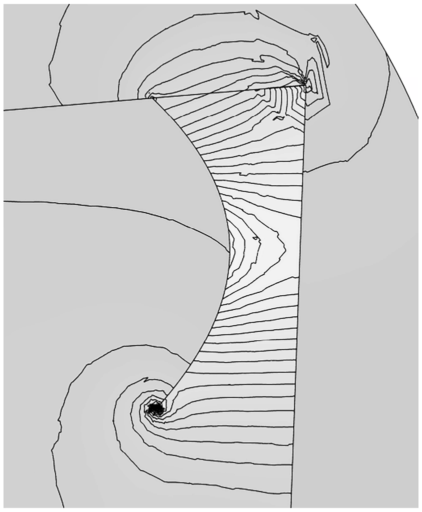

Figure 12. Velocity contour of Flared port at tuning frequency 52.5 Hz from COMSOL

As per Figure [12], gradual area increase reduces exit velocity, minimizing eddies, but abrupt flares at the entrance cause small eddies. Using fillets can mitigate this, enhancing smoother airflow and reducing vent noise.

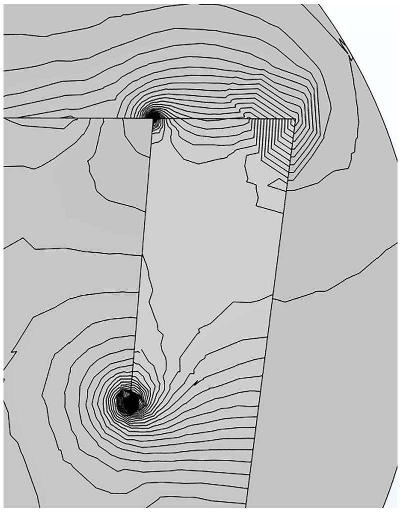

Figure 13. Velocity contour of Straight port at tuning frequency 65.5 Hz from COMSOL

Since the straight port from Figure [13] has sharp edges with abrupt changes in diameter, it is more prone to eddy formation. As air moves through the straight port, especially at high velocities, the sudden change in pressure and velocity when it meets external air can create turbulent flow at the exit. This turbulence can lead to increased noise (port noise) and potentially reduce the efficiency of the bass output due to energy loss in forming and dissipating these eddies.

As per Bezzola [16], increasing the port's flare angle shifts particle velocity from concave to convex at the exit. Flared ports show nearly flat velocity contours, reducing flow separation and turbulence, thus enhancing bass response and reducing distortion.

Working Prototype

The following detailed configuration was implemented for the experimental setup, particularly examining the impact of vent shapes. The vent shape was 3D printed using (ABS) plastic. This material was chosen for its durability and ease of printing complex geometries.

Figure 14. 3D printed flared vent installed on Wooden Cabinet prototype

Two identical subwoofer enclosures, each with an internal volume of 30 liters, were constructed from 15 mm thick Birch Plywood, known for its high quality and acoustic properties. One cabinet had a traditional straight wooden port measuring 7 inches long, Figure [16], while the second housed the 3D-printed vent, Figure [14].

Both cabinets were subjected to identical testing conditions to compare their acoustic outputs. An APx515 audio Analyzer generated the signals, and an ART SLA1 Studio Linear Amplifier powered the prototypes. The impedance of the straight-ported prototype (7 inches) was measured and tuned to 65.5 Hz, Figure [15].

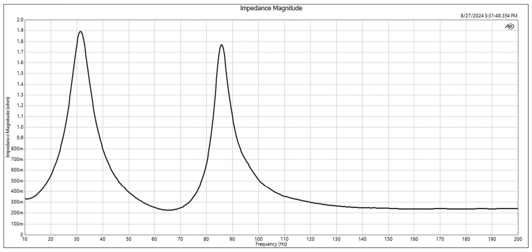

Figure 15. Straight vent Impedance measurement by APx515 Analyzer

In contrast, the 7-inch flared port prototype tuned to 52.5 Hz, Figure [8] demonstrates that a flared port achieves a lower tuning frequency than a straight port of equal length but with a smaller cross-section, even though the entrance and exit cross-section areas remain the same.

Figure 16. Straight wooden vent installed on Wooden Cabinet prototype

Vent Velocity Comparison

The vent velocities of the two subwoofer prototypes, one equipped with a 3D-printed port and the other with a straight wooden port, were measured using a digital anemometer. Both prototypes were driven by an ART SLA1 Studio Linear Amplifier. A voltmeter was connected directly to the amplifier's output to assess the electrical input accurately, facilitating precise voltage measurements.

Vent Velocities of both prototypes at the exit are measured using an Anemometer, with varying voltage measured by a Voltmeter, Figure [18]. Both port designs exhibit minimal air velocity at low voltages, Figure [17], with the flared port demonstrating a marginally higher velocity gradient. This suggests a lower resistance to airflow, potentially due to the gradual expansion of the port, which minimizes abrupt changes in air pressure.

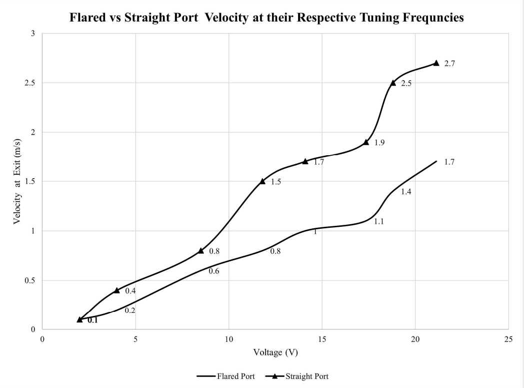

Figure 17. Straight port prototype APx515 Impedance

When moving to the medium-voltage zones, the flared port shows a steeper velocity gradient as voltage increases. This indicates an enhanced ability to accommodate higher airflow rates, likely due to the flared design's aerodynamic advantage, which reduces flow separation and thus decreases drag.

The flared port's air velocity gradient significantly outpaces the straight port's at high voltages. This performance gap highlights the flared port's capacity to maintain laminar flow at higher air speeds, which is crucial for preventing turbulence-induced noise (chuffing) at elevated sound pressure levels, a critical practical advantage.

Figure 18. Voltmeter (left) and Anemometer (right) used for measuring Voltage and Air velocity

Conclusions

Vent Geometry Impact: The geometry of the vent, including its flare and length, plays a significant role in influencing noise generation and propagation. Flared ports show improved performance over straight ports by reducing flow separation and turbulence.

Asymmetric Flared Ports: Despite their geometric challenges, asymmetric vent designs effectively achieve lower tuning frequencies and reduce vent noise compared to traditional straight ports. They can be tuned effectively using the minimum throat diameter for length correction, offering a practical solution when internal space constraints prevent traditional symmetric ports.

Prototype Validation: Experimental validation using 3D-printed prototypes confirmed that flared ports achieve a lower tuning frequency and better airflow management than straight ports, reducing port noise and improving bass response.

COMSOL Simulation Efficacy: COMSOL Multiphysics simulations and lumped speaker models effectively predicted acoustic behaviors. The simulations closely matched the experimental impedance measurements, validating the simulation model's ability to predict real-world acoustic behavior in vented loudspeaker systems.

References

1. Roozen, N. B., Bockholts, M., van Eck, P., and Hirschberg, A., "Vortex sound in bass-reflex ports of loudspeakers. Part I. Observation of response to harmonic excitation and remedial measures," *The Journal of the Acoustical Society of America*, 104(4), pp. 1914–1918, 1998, ISSN 0001-4966, doi:10.1121/1.423760.
2. Roozen, N. B., Vael, J. E. M., and Nieuwendijk, J. A., "Reduction of Bass-Reflex Port Nonlinearities by Optimizing the Port Geometry," in *Audio Engineering Society Convention 104*, Amsterdam, 1998.
3. Roozen, N. B., Bockholts, M., van Eck, P., and Hirschberg, A., "Vortex sound in bass-reflex ports of loudspeakers. Part II. A method to estimate the point of separation," *The Journal of the Acoustical Society of America*, 104(4), pp. 1919–1924, 1998, ISSN 0001-4966, doi:10.1121/1.423762.
4. Backman, J., "The nonlinear behavior of reflex ports," in *Audio Engineering Society Convention* 98, Paris, (1995)
5. Vanderkooy, J., "Nonlinearities in Loudspeaker Ports," in *Audio Engineering Society Convention* 104, Amsterdam, (1998)
6. Vanderkooy, J., "Loudspeaker Ports," in *Audio Engineering Society Convention* 103, New York City, (1997)
7. Uno Ingard, Hartmut Ising; "Acoustic Nonlinearity of an Orifice," *The Journal of the Acoustical Society of America,* 1 July 1967; 42 (1): 6–17.
8. García, Claudia. "Kármán vortex street in incompressible fluid models." *Nonlinearity* 33.4 (2020): 1625.
9. Salvatti, A., Devantier, A., and Button, D. J., "Maximizing performance from loudspeaker ports," *Journal of the Audio Engineering Society*, 50(1-2), pp. 19–45, (2002)
10. Sagers JD, Leishman TW, Blotter JD. "An extended lumped-element model and parameter estimation technique to predict loudspeaker responses with possible surround-dip effects". *J Acoust Soc Am.* 2013 Nov;134(5):3580-93. doi: 10.1121/1.4820886. PMID: 24180769.
11. "COMSOL Multiphysics v. 6.2," 2024.
12. "Lumped Loudspeaker Driver Using a Lumped Mechanical System" *https://www.comsol.com/model/lumped-loudspeaker-driver-using-a-lumped-mechanical-system-55901*
13. "LspCAD v. 5.25," 2024
14. "IronCAD" 2024
15. "Audio Precision APx515 Audio Analyzer"
16. Bezzola, A., "Optimal Bass Reflex Loudspeaker Port Design," in *COMSOL Conference*, Boston, 2019.

Acknowledgments

Yorkville Sound and Long and McQuade supported this work. The author would like to thank the co-author Todd Michael, Head of Yorkville Sound's Audio Lab, who helped with all aspects of this research, offered insightful suggestions, and contributed to it.